

Controlling for Cold Nuclear Matter Effects in Upsilon Production at the CMS detector via R_{pA} Analysis

Maine Christos

UC Davis Physics REU Program

August 2017

Abstract

The CMS experiment at the Large Hadron Collider (LHC) offers the possibility of studying the Quark Gluon Plasma (QGP) by measuring the rates of suppression of mesons made of heavy-flavored quarks. In this analysis, we attempt to study the suppression caused by Cold Nuclear Matter (CNM) effects through an R_{pA} analysis. We compare the rates of suppression of the Upsilon meson in proton-proton (pp) and proton-lead (pPb) collisions and calculate fits that are used to obtain the yields and then correct for efficiency and acceptance in each collision system. From these quantities, we can then quantify the amount of suppression we observe by calculating the nuclear modification factor (R_{pA}).

1 Introduction

The QGP is a strongly interacting plasma formed at the high energies produced by heavy-ion collisions at the LHC and is composed of dissociated quarks and gluons. The QGP will only form at high energies (150-170 MeV) due to a property of the strong force called asymptotic freedom, which causes the coupling constant of the strong force to decrease with increasing energy. Numerical calculations of Quantum Chromodynamics predict that the phase transition where hadrons dissociate to form the QGP occurs at an energy of 170 MeV.

Since the QGP is a strongly interacting plasma, we must use a strongly interacting particle to probe it. The particle used in this analysis is the Upsilon meson, which is a meson composed of one bottom and one anti-bottom quark. It has a ground state $\Upsilon(1S)$ with a mass of 9.46 GeV and two excited states $\Upsilon(2S)$ and $\Upsilon(3S)$ with masses of 10.0 GeV and 10.4 GeV respectively (using natural units). In a collision which produces both the QGP and an Upsilon meson, we expect that there will be a screening effect between the color charges in the plasma and the color charges in the quarks which make up the Upsilon. This will cause the meson to dissociate before it can reach our detector. The observable result of this effect is a suppression in the total number of Upsilon mesons we observe in our detector. By studying the rates of Upsilon mesons with and without the presence of the QGP, we can indirectly study the effects of the QGP.

We also expect to observe a suppression on Upsilon yields from Cold Nuclear Matter (CNM) effects. CNM effects can be thought of as the effects on the products of a collision due to processes within the colliding nucleus or nuclei which cannot be attributed to the QGP. These effects may occur in collisions where a proton collides with a Pb nucleus (pPb) and in collisions where a Pb nucleus collides with another Pb nucleus (PbPb) but will not occur for a collision where a proton collides with another proton (pp) since no heavy nuclei are present in pp collisions. The four main effects include Shadowing, Nuclear Absorption, energy loss of the parton (a parton is a quark or gluon) as it traverses the nucleus before the collision, and dissociation of the meson due to interactions with other hadrons produced during the collision. Shadowing is an effect which arises from the fact that the Parton Distribution Functions (PDFs) of nucleons

bound in a nucleus are different than a superposition of individual nuclei would predict. Nuclear Absorption occurs when a bound quark anti-quark state breaks up due to interactions within the nucleus[1]. These effects together result in additional suppression to Upsilon production in collisions where CNM is a factor. We only expect approximately 20% modification due to CNM effects whereas we expect the effects of the QGP to modify Upsilon yields by anywhere from a factor of 2 for the $\Upsilon(1S)$ state to a factor of 10 for the $\Upsilon(3S)$ state. However, despite the effects of the QGP being much larger than CNM effects, we still must find a way to isolate these effects to accurately measure the effects of the QGP in collisions where both are present (whereas CNM effects may be observed in pPb and PbPb collisions, the QGP is mostly observed in PbPb collisions). Therefore, we analyze Upsilon production in pPb collisions as a control experiment to understand the mechanisms of suppression present in cold nuclear matter.

2 The Detector

The LHC, located at CERN in Geneva, Switzerland, accelerates protons and heavy nuclei to nearly the speed of light and the collides them to produce the high energy conditions necessary to form the plasma. We analyze data from the CMS detector, one of four detectors at the LHC. The CMS detector is a superconducting solenoid with a magnetic field of 3.8 T and contains a silicon pixel and strip tracker, an electromagnetic calorimeter (ECAL), a hadronic calorimeter (HCAL), and muon chambers.

3 Types of Collisions

We observe three different types of collisions at the LHC: pp, pPb, and PbPb. In pp collisions where there are only two nucleons colliding with one another, there are not enough collisions to produce the QGP, nor do we have a nucleus which could produce CNM effects. For this reason, we call pp collisions the “pp reference” and use them as a baseline measurement to which we compare all other datasets. In pPb collisions, we still do not have enough nucleon-nucleon collisions to produce the QGP but we do observe CNM effects due to the Pb nucleus. We therefore call pPb collisions our “control experiment”. In PbPb collisions, we have enough nucleon-nucleon collisions to observe the QGP and we also observe CNM effects due to the presence of the Pb nuclei. Since the effects of the QGP are most prominent in PbPb collisions which are also affected by CNM effects, studying the QGP means we must separate the effects of QGP on Upsilon suppression from the effects of CNM on Upsilon suppression. Since only CNM effects are observed in pPb collisions, studying pPb collisions allows us to quantify the level of modification that can be attributed to CNM effects.

We use pp collisions as our reference experiment as we don’t expect the QGP to be produced in these collisions. To calculate the number of Upsilon we would expect in a PbPb collision if no QGP is produced, we scale the number of Upsilon produced by the average number of collisions we can expect given the number of nucleons in a Pb nucleus. We then compare this number to the number we have observed in data to measure the suppression of the Upsilon.

4 Methods

4.1 The Invariant Mass of the Upsilon

We reconstruct the Upsilon meson exclusively through its dimuon decay channel, where the Upsilon meson decays into two oppositely-charged muons. Since the Upsilon decays before it reaches the detector, we measure only the muons which have been produced by an Upsilon decay and not the Upsilon itself. We can check if a dimuon originated from an Upsilon decay by adding the 4-momentum of the two muons and then taking the invariant mass of their combined 4-momentum. If the invariant mass is the same as that of the Upsilon, we say we have observed an Upsilon candidate. We choose to study the dimuon decay channel of the Upsilon due to

the geometry of our detector. Since heavy ion collisions produce many hits in the tracker and calorimeters of the detector, it can be difficult to reconstruct the particles produced in the collision. However, a muon pair will have enough momentum to pass through the tracker and calorimeters and will be observed as two isolated muons in the muon chambers.

4.2 Efficiencies

Since not every particle produced in a given collision will make it to the detector, we calculate the efficiency of a particle to be observed in our detector. We define the efficiency as:

$$\epsilon = \frac{\text{Reconstructed dimuons passing analysis cuts}}{\text{Generated dimuons passing acceptance cuts}} \quad (1)$$

The number of generated dimuons refers to the number of muons decaying from an Upsilon in our Monte Carlo simulations before the muons hit the detector. The number of reconstructed dimuons is defined as the number of dimuons that have decayed from an Upsilon, hit the detector, interacted with the materials in the detector and are reconstructed in our simulation. The analysis and acceptance cuts are additional requirements that we place on the kinematics of the muons which include constraints on their momentum in the plane transverse to the collision (p_T) and their rapidity (y), a quantity associated with their momentum in the longitudinal direction. We also weight the efficiencies using data-driven methods which include p_T Re-weights and Tag and Probe weights. We calculate these efficiencies for different ranges or “bins” of variables p_T and rapidity. Efficiencies for the $\Upsilon(3S)$ state for pPb are omitted until a new Monte Carlo simulation for the $\Upsilon(3S)$ is generated.

4.3 The Nuclear Modification Factor

The Nuclear Modification Factor allows us to quantify the suppression of Upsilon mesons due to the QGP and CNM effects. R_{pA} is the nuclear modification factor for proton-nucleus collisions (eg. pPb collisions) and is expressed as:

$$R_{pA} = \frac{N_{pA} \cdot \epsilon_{pp}}{\langle N_{Coll} \rangle \cdot N_{pp} \cdot \epsilon_{pA}} \quad (2)$$

Where N_{pA} is the number of Upsilon mesons produced in pPb collisions, N_{pp} is the number of Upsilon mesons produced in pp collisions, $\langle N_{Coll} \rangle$ is the average number of nucleon-nucleon collisions in a pPb collision, ϵ_{pA} is the efficiency of pPb collisions and ϵ_{pp} is the efficiency of pp collisions. The R_{pA} is a measure of CNM Effects only. The nuclear modification factor for PbPb collisions is expressed as:

$$R_{AA} = \frac{N_{AA} \cdot \epsilon_{pp}}{\langle N_{Coll} \rangle \cdot N_{pp} \cdot \epsilon_{AA}} \quad (3)$$

Where N_{AA} is the number of Upsilon mesons produced in PbPb collisions, N_{pp} is the number of Upsilon mesons produced in pp collisions, $\langle N_{Coll} \rangle$ is the average number of nucleon-nucleon collisions in a PbPb collision, ϵ_{AA} is the efficiency of PbPb collisions and ϵ_{pp} is the efficiency of pp collisions. The R_{AA} is a measure of both CNM and QGP effects.

4.4 Yields

In order to calculate the total number of Upsilon mesons we have observed, we fit our data using a sum of functions to represent the three peaks of the Upsilon mesons and the background (background includes any opposite dimuons in the mass range of the Upsilon which did not actually originate from an Upsilon). Each Upsilon meson peak is represented by a signal model parameterized by a double Crystal-ball function (A double Crystal-ball function resembles a

Gaussian with extra weight in the low energy tail). The background is modeled by an error function multiplied by an exponential. We first fit the function to a Monte-Carlo simulation and then use the parameters from the simulation fit to seed the fit function when we fit it to the data. Once we have fit our combined signal and background functions to the data, we subtract the background function to obtain the Upsilon yields.

To be sure that our fitting code is working properly, we first reproduce fitting the results of pp collisions from a previous analysis which used a PbPb dataset instead of a pPb dataset[2]. This analysis used a slightly different binning scheme where the variable y ranges from $-2.4 < y < 2.4$ for the PbPb dataset instead of $-1.93 < y < 1.93$ for the pPb dataset.

5 Results

5.1 Efficiencies

Efficiencies for pp were calculated for $p_T < 30$ and $|y| < 1.93$.

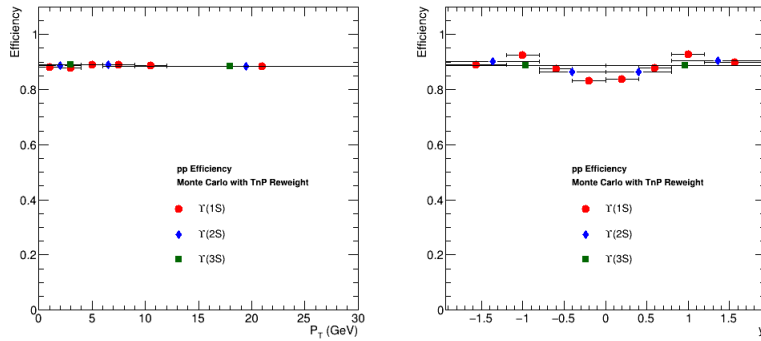


Figure 1: Efficiencies calculated for pp for the $\Upsilon(1S)$ (red circles), $\Upsilon(2S)$ (blue diamonds), and $\Upsilon(3S)$ (green squares) states binned by transverse momentum (left) and rapidity (right).

Efficiencies for pPb were calculated for $p_T < 30$ and $|y| < 1.93$ in the same bins as efficiencies for pp. Efficiencies for $\Upsilon(3S)$ are excluded as mentioned earlier.

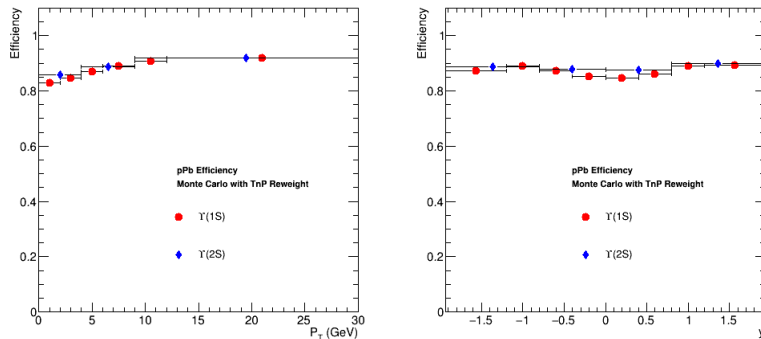


Figure 2: Efficiencies calculated for pPb for the $\Upsilon(1S)$ (red circles) and $\Upsilon(2S)$ (blue diamonds) states binned by transverse momentum (left) and rapidity (right).

5.2 Fits

First, fits are calculated for bins from the older analysis with $|y| < 2.4$. We then compare our fits to the previous results to verify that our code is functioning properly. A comparison of the yields calculated is shown in Figure 3 and a subset of the bins which were compared are shown in Figure 4.

| p_T Range ($\Upsilon(1S)$) | Previous Fit | Our Reproduced Fit |
|--------------------------------|--------------|--------------------|
| 0-2 GeV | 6689 | 6689 |
| 2-4 GeV | 6993 | 6698 |
| 4-6 GeV | 6353 | 6343 |
| 6-9 GeV | 6696 | 6758 |
| 9-12 GeV | 4054 | 4144 |
| 12-30 GeV | 4509 | 4452 |

| p_T Range ($\Upsilon(2S)$) | Previous Fit | Our Reproduced Fit |
|--------------------------------|--------------|--------------------|
| 0-4 GeV | 3917 | 3915 |
| 4-9 GeV | 4018 | 4067 |
| 9-30 GeV | 3085 | 3031 |

| p_T Range ($\Upsilon(3S)$) | Previous Fit | Our Reproduced Fit |
|--------------------------------|--------------|--------------------|
| 0-6 GeV | 2937 | 2669 |
| 6-30 GeV | 3024 | 3073 |

| y Range ($\Upsilon(1S)$) | Previous Fit | Our Reproduced Fit |
|------------------------------|--------------|--------------------|
| 1.6-2.0 | 5496 | 5684 |
| 1.6-2.4 | 7422 | 7441 |
| 1.2-2.4 | 14039 | 14035 |

| y Range ($\Upsilon(2S)$) | Previous Fit | Our Reproduced Fit |
|------------------------------|--------------|--------------------|
| 1.6-2.0 | 1692 | 1683 |
| 1.6-2.4 | 2410 | 2310 |
| 1.2-2.4 | 4379 | 4368 |

| y Range ($\Upsilon(3S)$) | Previous Fit | Our Reproduced Fit |
|------------------------------|--------------|--------------------|
| 1.6-2.0 | 884 | 928 |
| 1.6-2.4 | 1198 | 1201 |
| 1.2-2.4 | 2262 | 2260 |

Figure 3: Tables showing previously calculated yields with our calculation for bins in p_T and y used for the $\Upsilon(1S)$, $\Upsilon(2S)$, and $\Upsilon(3S)$.

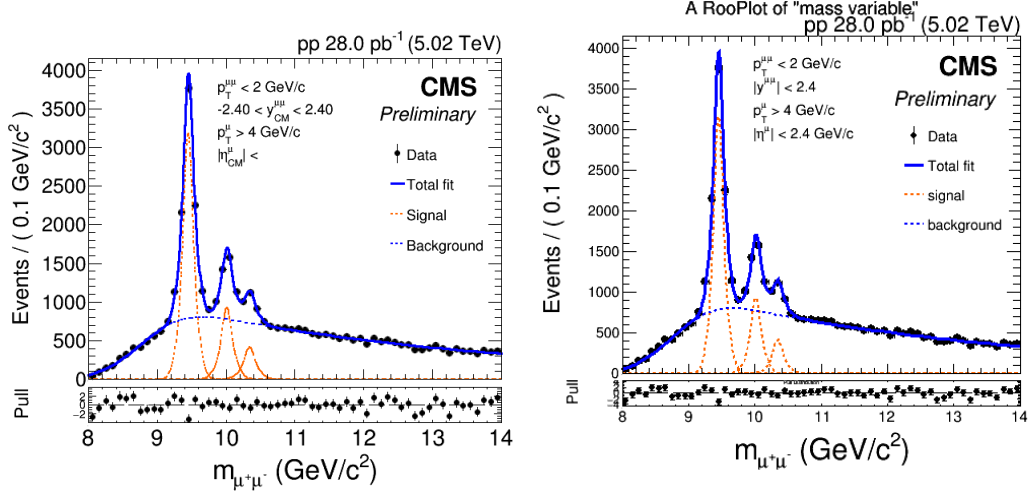


Figure 4: Fits calculated in our analysis using the bins of previous analysis (left) compared to fits calculated in old analysis (right).

All fits appear to match reasonably well. We then perform fits to be used in the R_{pA} calculation, where we measure in the rapidity range $|y| < 1.93$ for the pPb dataset. The rapidity range for pPb is smaller than for PbPb due to a boosting which occurs in PbPb collisions. A subset of two of these fits for pp are shown in Figure 5.

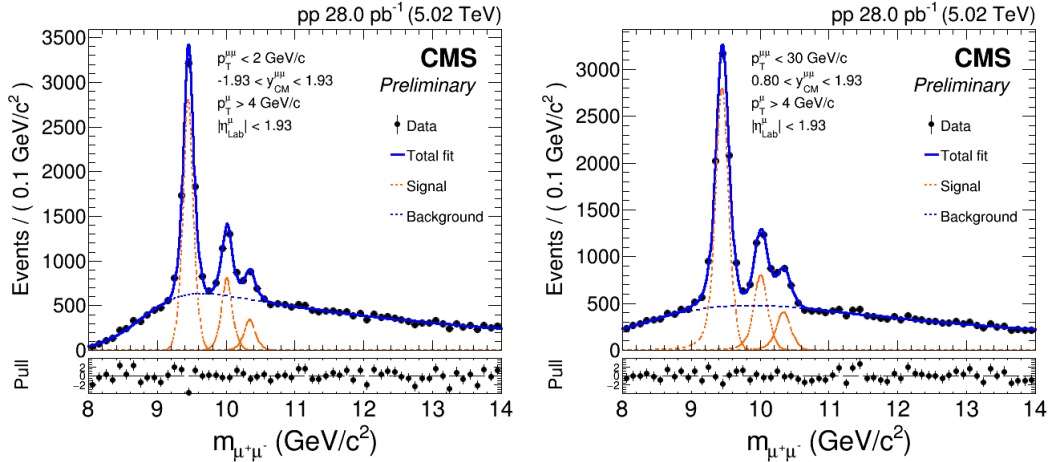


Figure 5: Fits calculated for pp collisions with $|y| < 1.93$

The pp fits were calculated from fits which were seeded with values obtained by fitting first to Monte Carlo. The pull distributions in the bottom panel of the fits are reasonable with most datapoints lying within 2-3 standard deviations of the fit and with low χ^2/dof .

Finally, we perform fits for the pPb dataset using the rapidity range $|y| < 1.93$. As no pPb fits were used in the previous analysis, the fits and the yields which we extract from them are a new result for this dataset. A subset of two of these fits are shown in Figure 6.

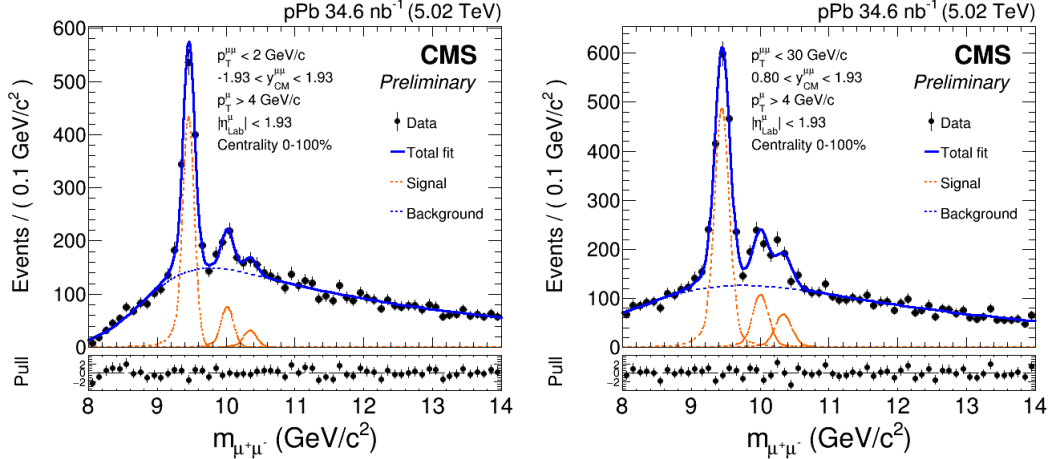


Figure 6: Fits calculated for pPb collisions with $|y| < 1.93$

Unlike our fits for pp collisions, our pPb fits were calculated by fitting directly to the data rather than fitting first to Monte Carlo Simulation and then seeding the fit before fitting to the data. The goodness of the fits were calculated using a χ^2 test and the fits appear to match the data as is shown by the agreement of the pull distribution in the bottom panels. The largest χ^2/dof of any of the fits is 1.35.

5.3 R_{pA}

The R_{pA} values for the p_T and Rapidity bins mentioned earlier have not yet been calculated; however, this step is relatively simple and will be completed soon as the yields and efficiencies have now been calculated.

6 Conclusion and Future Directions

The yields of Upsilon were calculated and match those calculated in a previous analysis. New yields of Upsilon with efficiencies were also successfully calculated for pp data. We also calculated efficiencies for the $\Upsilon(2S)$ and $\Upsilon(3S)$ states of the Upsilon in pPb collisions. Finally, we calculated fits and obtained yields for all 3 states of the Upsilon in the pPb dataset. Efficiencies were about 80-90% for all p_T and rapidity bins. Fitting parameters for pPb were obtained by fitting directly to the data.

In the future, we hope to attempt a fitting procedure where we fit first to the simulation before fitting to the data when calculating pPb yields. We hope that this method and others will allow us to calculate systematic uncertainties for pPb. We also hope to finish calculating R_{pA} for pPb data in the new rapidity bins. Once we have more complete simulations, we can also choose to bin in high vs. low event activity. We will also apply correction factors as necessary to the pp dataset bins to account for difference in rapidity range used in pPb vs. PbPb collisions.

7 Acknowledgements

Thank you to the UC Davis REU Program, Dr. Rena Zieve, and the NSF for making this project possible. All work was done in close collaboration with UC Davis Nuclear Physics Group under Dr. Manuel Calderón. Thank you to Santona Tuli, Ota Kukral, and Dr. Calderón for all their help and guidance with this work.

8 References

- [1] Santana Tuli. Quarkonia Analysis of Ultra-Relativistic Heavy-Ion Collisions with the CMS Detector, 2016.
- [2] Yongsun Kim, Jaebeom Park, Dongho Moon, Geonhee Oh, Chad Flores. Nuclear Modification Factor of $\Upsilon(nS)$ in PbPb Collisions at $\sqrt{s}=5.02$ TeV, 2016.